

## ARTICLE OPEN



# Enhancing venetoclax efficacy in leukemia through association with HDAC inhibitors

Jorge Antonio Elias Godoy Carlos<sup>1</sup>, Mauricio Temotheo Tavares<sup>2,3,4</sup>, Keli Lima<sup>1,5</sup>, Larissa Costa de Almeida<sup>1</sup>, Karoline de Barros Waitman<sup>2</sup>, Leticia Veras Costa-Lotufo<sup>1</sup>, Roberto Parise-Filho<sup>2</sup> and João Agostinho Machado-Neto<sup>1</sup>✉

© The Author(s) 2025

Epigenetic modifications significantly influence gene expression and play crucial roles in various biological processes, including carcinogenesis. This study investigates the effects of novel purine-benzohydroxamate compounds, particularly **4f**, as hybrid kinase/histone deacetylase (HDAC) inhibitors in hematological malignancies, focusing on acute myeloid leukemia (AML). Our results demonstrate that these compounds selectively reduce cell viability in blood cancer cells, with inhibitory concentration values indicating higher potency against neoplastic cells compared to normal leukocytes. Mechanistically, **4f** induces apoptosis and cell cycle arrest, promoting differentiation in leukemia cells, while effectively inhibiting HDAC activity. Furthermore, **4f** enhances the therapeutic efficacy of venetoclax, a BCL2 inhibitor, in AML models sensitive and resistant to this drug. The combination treatment significantly increases apoptosis and reduces cell viability, suggesting a synergistic effect that may overcome drug resistance. This study provides valuable insights into the potential of HDAC inhibitors, particularly **4f**, as a promising therapeutic strategy for treating resistant hematological malignancies. Our findings underscore the importance of further exploring hybrid kinase/HDAC inhibitors in combination therapies to improve outcomes in patients with acute leukemias and other hematological malignancies.

*Cell Death Discovery* (2025)11:147; <https://doi.org/10.1038/s41420-025-02446-4>

## INTRODUCTION

Epigenetic modifications are heritable changes that modulate the chromatin structure without altering the DNA nucleotide sequence. In humans, epigenetic alterations play a crucial role in regulating gene expression, and various types of these modifications have been extensively documented. The most well-characterized epigenetic modifications include DNA methylation, histone modifications, and non-coding RNAs [1–3]. Among these, the acetylation and deacetylation of histones are post-translational modifications that have been widely studied, playing a key role in chromatin remodeling. This process is regulated by two enzyme families: histone acetyltransferases (HATs) and histone deacetylases (HDACs), which add or remove acetyl groups from the  $\epsilon$ -amino groups of histone lysine residues, leading to either an open or condensed chromatin structure, thereby promoting gene expression or repression, respectively [4, 5].

The acetylation process mediated by HATs opens the chromatin, allowing the expression of genes involved in processes such as cell cycle progression, apoptosis, and autophagy, which are relevant to carcinogenesis. Conversely, HDACs exert a repressive effect by reducing histone acetylation through the removal of acetyl groups from lysine residues, leading to chromatin condensation and gene repression [6–8]. HDAC inhibitors (HDACi) have been clinically used, either as monotherapy or in combination with other antineoplastic drugs. Numerous clinical trials have

investigated various HDACi, offering new perspectives in the treatment of cancer [9, 10].

HDACi have been extensively investigated in hematological malignancies, particularly in acute leukemias, which are diseases with poor prognosis and difficult therapeutic management [11]. In these models, it has been frequently reported that HDAC inhibition leads to histone hyperacetylation, resulting in chromatin decompaction and reactivation of tumor suppressor and differentiation genes [12, 13]. Another important aspect is that, in acute leukemias, HDACi have been mainly studied in combination with other therapies. HDACi monotherapies generally show limited efficacy, but when combined with agents such as DNA methyltransferase inhibitors, targeted therapies, or conventional chemotherapeutics, they demonstrate synergistic potential [14–16]. In this context, the use of HDACi with dual-targeting capabilities may be of interest, as this pharmacological property could offer advantages in overcoming the issues of non-selectivity and drug resistance commonly associated with single-target therapies [17, 18]. Thus, the use of HDACi in acute leukemias is still being refined, focusing on therapeutic combinations and the identification of biomarkers that could predict which patients would benefit most from this type of treatment.

In the present study, we characterized the cellular and molecular effects of novel hybrid kinase/HDAC inhibitors [19], as well as evaluated their combination with venetoclax, a BCL2

<sup>1</sup>Department of Pharmacology, Institute of Biomedical Sciences, University of São Paulo, São Paulo, Brazil. <sup>2</sup>Department of Pharmacy, Faculty of Pharmaceutical Science, University of São Paulo, São Paulo, Brazil. <sup>3</sup>Department of Cancer Biology, Dana-Farber Cancer Institute, Boston, MA 02115, USA. <sup>4</sup>Department of Biological Chemistry and Molecular Pharmacology, Harvard Medical School, Boston, MA 02115, USA. <sup>5</sup>Laboratory of Medical Investigation in Pathogenesis and Targeted Therapy in Onco-Immunohematology (LIM-31), Department of Internal Medicine, Hematology Division, Faculty of Medicine, University of São Paulo, São Paulo, Brazil. ✉email: jamachadoneto@usp.br

Received: 16 November 2024 Revised: 12 March 2025 Accepted: 26 March 2025

Published online: 06 April 2025

inhibitor, in experimental models of acute myeloid leukemia (AML).

## RESULTS

### Purine-benzohydroxamate compounds drive selective reduction of cell viability in cellular models of hematological malignancies

As previously reported, a series of hybrid inhibitors combining pharmacophores from known kinase inhibitors and HDAC inhibitors were synthesized and initially tested on Jurkat and Namalwa cell lines [19]. In this study, we significantly expand upon these initial findings by evaluating the efficacy of these compounds across a broader panel of hematological malignancies, including cellular models of AML, ALL, MPN, lymphoma, and MM. As shown in Fig. 1A, the compound **4d** reduces cell viability with  $IC_{50}$  values ranging from 0.10 and 1.56  $\mu$ M, while **4e** shows  $IC_{50}$  values between 0.11 to 1.94  $\mu$ M, and **4f** exhibits  $IC_{50}$  values from 0.09 to 0.89  $\mu$ M in myeloid neoplasm models. In lymphoid neoplasms (Fig. 1B),  $IC_{50}$  values range from 0.13 to 2.21  $\mu$ M for **4d**, from 0.05 to 4.42  $\mu$ M for **4e**, and from 0.11 to 2.04  $\mu$ M for **4f**. Importantly, the compounds demonstrated significantly higher  $IC_{50}$  values in normal leukocytes (Fig. 1C), suggesting selective cytotoxicity toward neoplastic cells (selective index ranged from 2.21 to >555-fold). Vorinostat, used as a reference drug, exhibited  $IC_{50}$  values ranging from 0.27 to 1.63  $\mu$ M in myeloid neoplasms, from 0.47  $\mu$ M to 4.21  $\mu$ M in lymphoid neoplasms, and >50  $\mu$ M in normal leukocytes. Given the more pronounced effects observed in myeloid neoplasms, we selected several molecularly distinct models for further investigation. These studies revealed that the reduction induced by the purine-benzohydroxamate compounds in cell viability was both time- and concentration-dependent ( $p < 0.05$ , Supplementary Fig. 1).

### Purine-benzohydroxamate compounds exhibit multiple antineoplastic effects in leukemia cells

Next, potential mechanisms involved in the reduction of cell viability induced by purine-benzohydroxamate compounds were investigated. Firstly, it was observed that the compounds triggered apoptosis, with **4f** being the most effective (Fig. 2 and Supplementary Fig. 2). Thus, we continued to deepen the characterization of **4f** in the following experiments. At low concentrations, **4f** causes a reduction in cell cycle progression with accumulation of cells in the  $G_0/G_1$  phases and a reduction in cells in the S,  $G_2/M$  phases. At higher concentrations, there is an accumulation of cells in sub $G_1$ , corroborating the data from the cell death assays (Fig. 3A, B). Autonomous colony formation assays revealed that **4f** is more effective than vorinostat, being able to completely inhibit clonogenicity in MOLM-13 and THP-1 cells (Fig. 3C, D).

Given that HDACs contribute as repressors of cell differentiation in AML models [13], we investigated the effects of **4f** on this process. In NB4-R2 and THP-1 cells, exposure to **4f** led to a significant increase in the cell differentiation marker CD11b, surpassing the effects of vorinostat (Supplementary Fig. 3A). Morphological analysis further revealed that **4f** altered the nuclei-to-cytoplasm ratio and increased vacuole formation, which are indicative of a more differentiated cell phenotype (Supplementary Fig. 3b).

### Compound **4f** reduces HDAC activity and favors a tumor suppressive molecular network in AML models

Exposure to **4f** modulated proteins involved in HDAC activity. Specifically, changes were observed in acetyl- $\alpha$ -tubulin (Lys40) and acetyl-histone H3 (Lys9), which are substrates of HDAC6 and HDAC class I, respectively. As shown in Fig. 4, leukemia cells exhibited increased levels of these acetylated proteins,

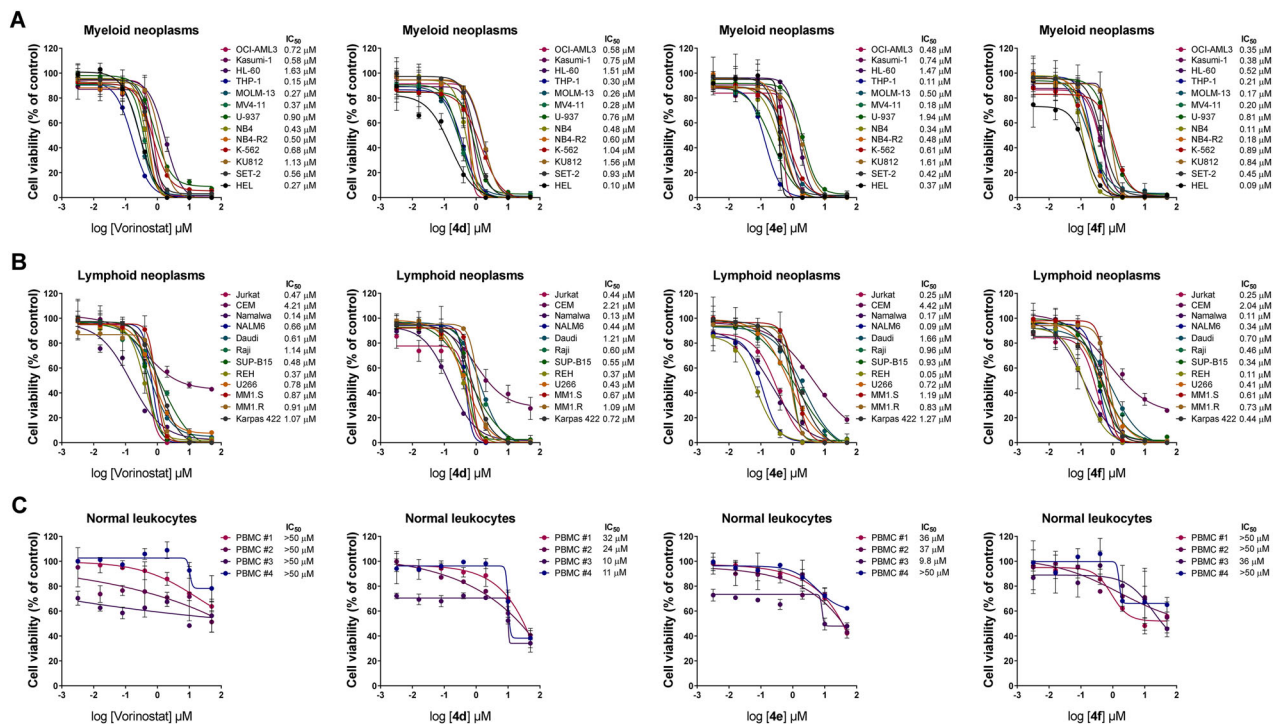


**Fig. 1** Purine-benzohydroxamate compounds selectively reduce cell viability, with compound **4f** being the most potent in blood cancer models tested. Dose- and time-dependent cytotoxicity was analyzed by methylthiazolotetrazolium (MTT) assay using 13 myeloid neoplasm cell lines (A), 12 lymphoid neoplasm cell lines (B), and 4 normal leukocyte samples (C) treated with vehicle or graded concentrations of vorinostat, **4d**, **4e**, or **4f** (ranging from 0.0032 to 50  $\mu$ M) for 72 h. Cell viability was measured as a percentage relative to vehicle-treated controls. Data are presented as mean  $\pm$  SD from at least three independent experiments.  $IC_{50}$  values for each compound and cellular model are described in the Figure.

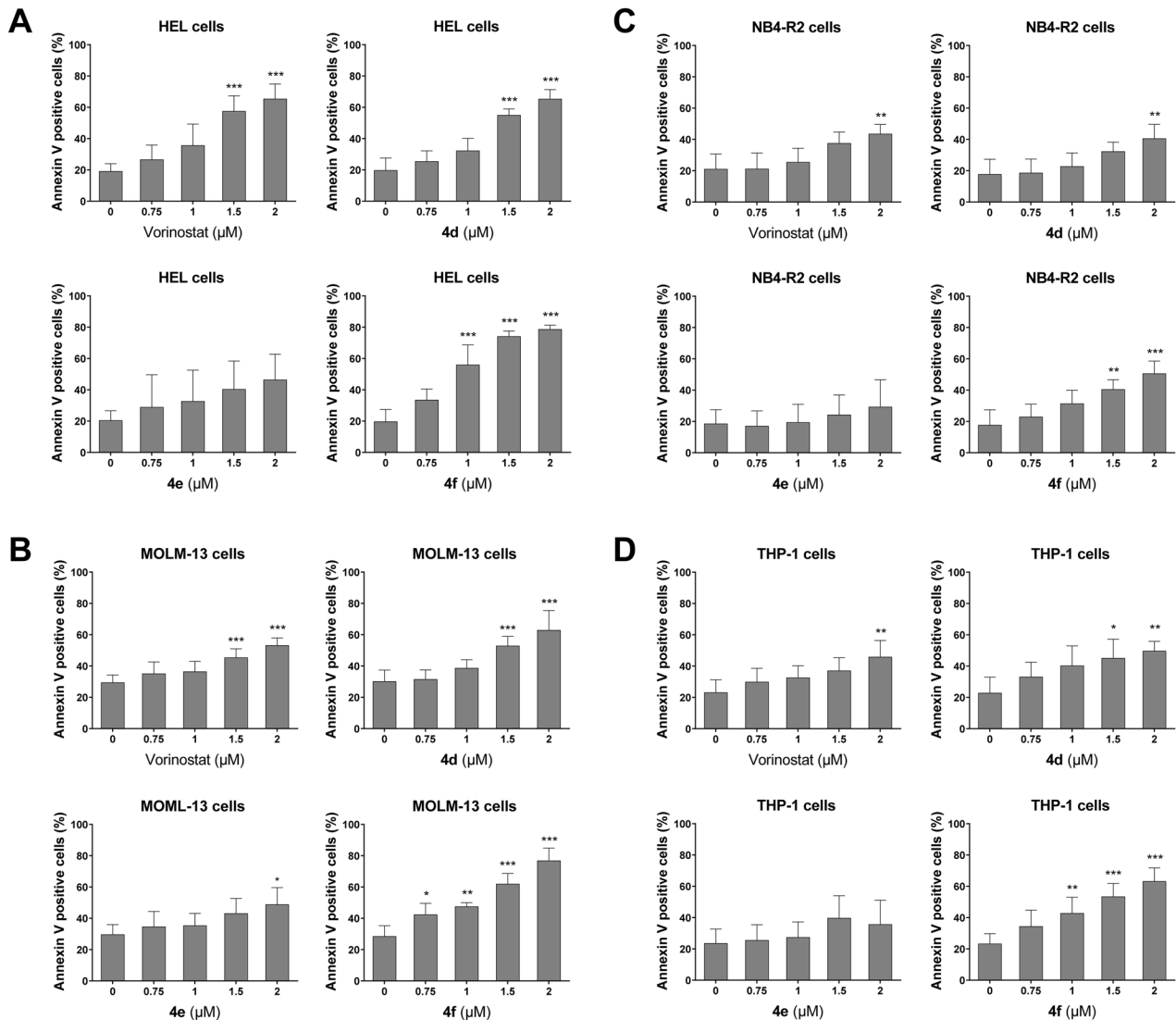


**Fig. 2** Novel HDAC inhibitors induce apoptosis in acute myeloid leukemia cells. HEL (A), MOLM-13 (B), NB4-R2 (C), and THP-1 (D) cells were labeled with APC-annexin V/propidium iodide (PI) after treatment with either vehicle or the indicated concentrations of vorinostat, **4d**, **4e**, or **4f** for 24 h. Bar graphs show the mean  $\pm$  SD of at least three independent experiments. The *p* values and cell lines are indicated in the graphs; \**p* < 0.05, \*\**p* < 0.01, \*\*\**p* < 0.0001; ANOVA and Bonferroni post-test.

indicating that the compound inhibits HDACs within 3 h of treatment.

Since HEL cells were more sensitive to **4f**, we selected this model for further molecular analyses. We investigated a broad panel of genes involved in cell cycle, apoptosis, DNA damage, and autophagy. Both vorinostat and **4f** modulated the genes *BNIP3*, *CCNB1*, *CCNA2*, and *MCL1* (Fig. 5A). Notably, HEL cells treated with **4f** showed a greater number of modulated genes compared to those treated with vorinostat. The biological processes and signaling pathways associated with vorinostat include cycle G<sub>2</sub>/M phase transition, regulation of cyclin-dependent protein kinase activity, mitochondrial membrane permeability involved in apoptotic process, signal transduction in response to DNA damage, and serine/threonine protein kinase complex. In contrast, **4f** was associated with pathways including serine/threonine protein kinase complex, G<sub>1</sub>/S transition of mitotic cell cycle, cell cycle arrest, macroautophagy, and DNA damage checkpoint (all FDR < 0.05, Fig. 5B).

#### HDAC inhibition by **4f** potentiates apoptosis-induced by venetoclax in AML cells

Given the potential of **4f** as an antileukemic agent, we sought to evaluate whether this compound could be a better drug for clinical use in acute leukemias. To further refine this strategy, we first evaluated HDAC expression in AML, and observed that *HDAC2*, *HDAC6*, and *HDAC8* are overexpressed in AML patients when compared to healthy donors (Supplementary Fig. 4). Using data from ex vivo assays of the AML cohort of the Beat AML study, we identified a set of drugs in which high expression of *HDAC2*, *HDAC6*, and *HDAC8* would be associated with therapy resistance, with venetoclax being recurrent for *HDAC2* and *HDAC6* (Supplementary Fig. 5). Given the relevance of venetoclax for AML therapy [20], we decided to further investigate the combination of HDAC inhibitors with venetoclax in AML models with drug resistance.

In HL-60 (venetoclax-sensitive), HEL and NB4-R2 cells (intrinsically resistant to venetoclax) the combination of vorinostat or **4f** with venetoclax potentiated the reduction in viability (Fig. 6A–C) and the induction of apoptosis in all models tested (Fig. 6D–F).

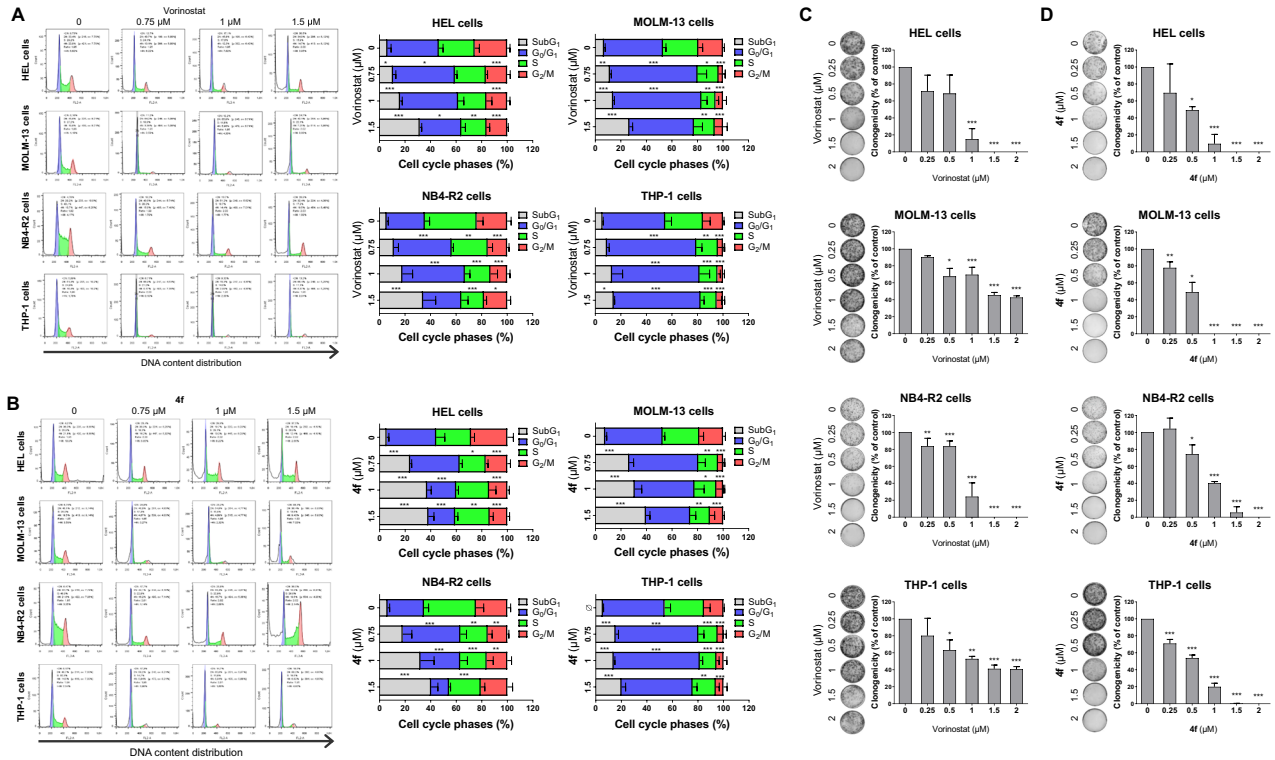


**Fig. 3** The novel HDAC inhibitor 4f induces cell cycle arrest and efficiently reduces autonomous clonal growth in acute myeloid leukemia (AML) cells. Cell cycle phases were determined by analyzing DNA content via propidium iodide staining, followed by data acquisition using flow cytometry after treating AML cells with either vehicle, vorinostat (A), or 4f (B) at the indicated concentrations for 24 h. A representative histogram is shown for each condition. The bar graph displays the mean  $\pm$  SD of at least three independent experiments. The  $p$  values and cell lines are indicated in the graphs; \* $p$  < 0.05, \*\* $p$  < 0.01, \*\*\* $p$  < 0.001; ANOVA and Bonferroni post-test. HEL, MOLM-13, NB4-R2, and THP-1 cells were cultured in a semisolid medium in the presence of either vehicle or increasing concentrations of vorinostat (C) or 4f (D). Colonies containing viable cells were detected by adding MTT reagent after 8–12 days of culture. Colony images are shown for a representative experiment, and the bar graphs display the mean  $\pm$  SD of at least three independent experiments. \* $p$  < 0.05, \*\* $p$  < 0.01, \*\*\* $p$  < 0.001; ANOVA and Bonferroni post-test.

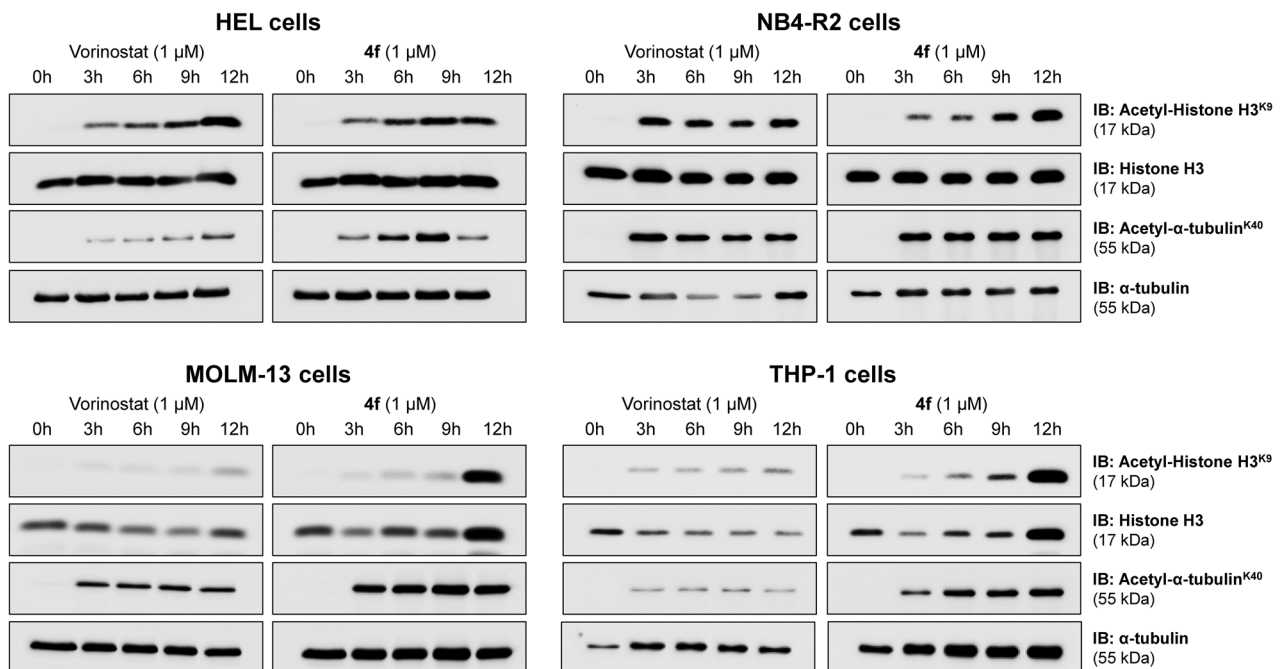
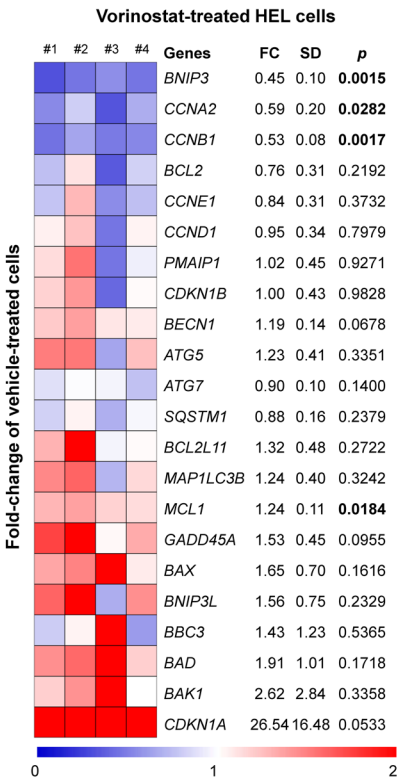


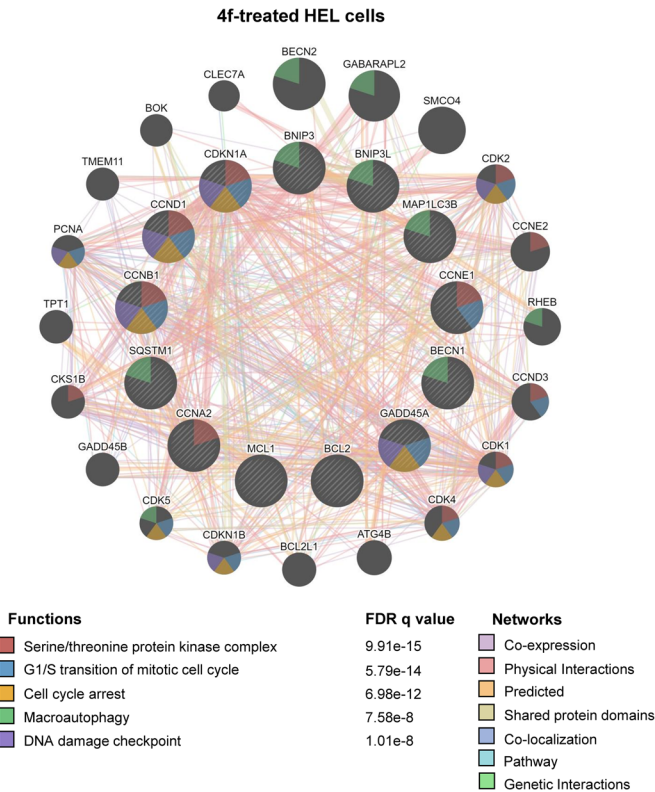
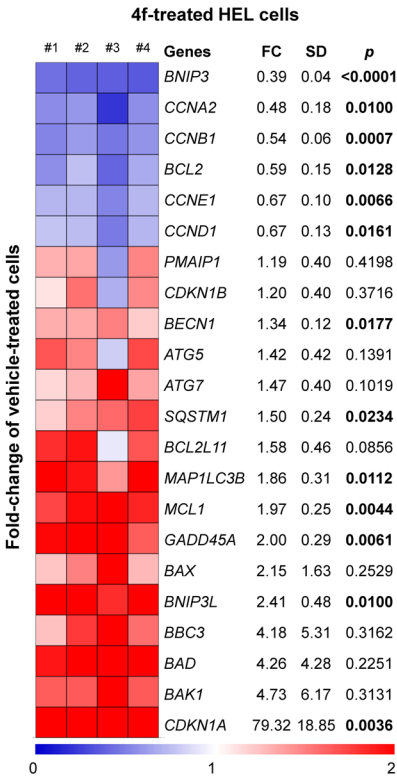
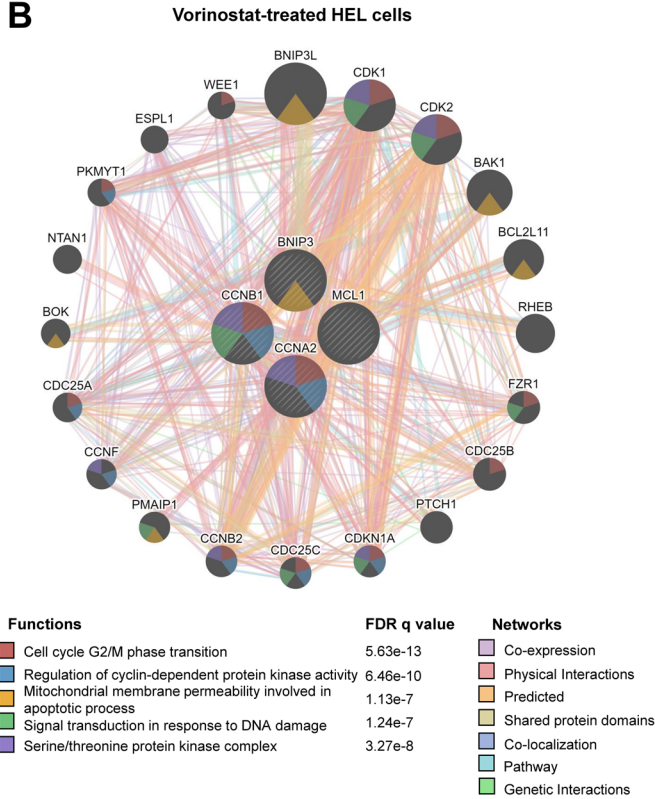
**Fig. 4** Compound 4f inhibits HDAC activity in acute myeloid leukemia cells. Western blot analysis was performed to detect acetyl-histone H3 (Lys9), histone H3, acetyl- $\alpha$ -tubulin (Lys40), and  $\alpha$ -tubulin in total cell extracts from HEL, NB4-R2, MOLM-13, and THP-1 cells treated with vehicle, vorinostat (1  $\mu\text{M}$ ), or 4f (1  $\mu\text{M}$ ) for 0, 3, 6, 9, or 12 h. Vorinostat was used as a reference drug. Cell lines are indicated in the Figure.



**A**



**B**



**DISCUSSION**

In the USA, the incidence of AML is approximately 4.3 per 100,000 people per year, with a median diagnosis age of 65–72 years in Western countries, making it the most common type of acute

leukemia among hematologic malignancies [21]. Treatment approaches are influenced by patient characteristics such as age, comorbidities, and performance status [22, 23]. It is crucial to determine the molecular profile of AML to select the most

**Fig. 5 HDAC inhibitors promote a molecular network associated with cell cycle arrest, autophagy, and DNA damage response in HEL cells.** **A** Quantitative PCR assay for a panel of key genes involved in proliferation, cell cycle progression, apoptosis, DNA damage, and autophagy was performed. The data presented represents the average of at least four independent experiments. Heatmap showing the gene expression profile of HEL cells treated with vehicle, vorinostat (1  $\mu$ M), or **4f** (1  $\mu$ M) for 24 h. Blue indicates decreased mRNA levels, while red indicates increased mRNA levels, normalized to vehicle-treated cells ( $n = 4$ ). Fold-change (FC) relative to vehicle-treated cells, standard deviation (SD), and  $p$  values are described using the Student's  $t$  test. **B** A gene network for vorinostat- or 4f-modulated genes was constructed using the GeneMANIA database (<https://genemania.org/>). Genes significantly modulated are represented as crosshatched circles, while interacting genes added by the software are shown as non-crosshatched circles. The main biological interactions, associated functions, and false discovery rate (FDR)  $q$ -values are detailed in the Figure.

appropriate treatment. Standard induction chemotherapy involves cytarabine combined with anthracyclines or alternative agents to achieve complete remission, followed by consolidation therapy, often including high dose cytarabine or hematopoietic stem cell transplantation in eligible patients. Unfortunately, older patients are typically not eligible for intensive chemotherapy, and only 30% of these patients survive for five years (excluding the acute promyelocytic leukemia subtype). Outcomes for relapsed/refractory AML patients are poor, with less than 10% overall survival over three years [22–25]. These concerning clinical outcomes underscore the pressing need for new therapies or drug combinations to improve the treatment efficacy of acute leukemias.

Here in, we explored the potential of novel hybrid kinase/HDAC inhibitors in a broad panel of blood cancers, both as monotherapy and in combination with venetoclax, a leading targeted therapy for AML [19, 26]. HDACs are a group of enzymes classified into four classes, responsible for deacetylating histones, and some types may deacetylate non-histone substrates. HDACs remove acetyl groups from the lysine tails of histones, restoring their positive charge, which creates a stronger interaction between histones and DNA (which carries a negative charge), resulting in more condensed chromatin and reduced access to transcription factors. Consequently, transcription of suppressor tumor-related genes is downregulated [27]. Multiple studies have demonstrated that histone modifications play a role in the pathogenesis of both solid tumors and hematologic malignancies, often associated with advanced disease and poor prognosis [27–31]. For example, in AML, HDACs are aberrantly recruited by oncogenic fusion proteins like PML::RAR $\alpha$ , PLZF::RAR $\alpha$ , or AML1::ETO, leading to gene silencing, which contributes to differentiation arrest and leukemogenesis [27–30, 32].

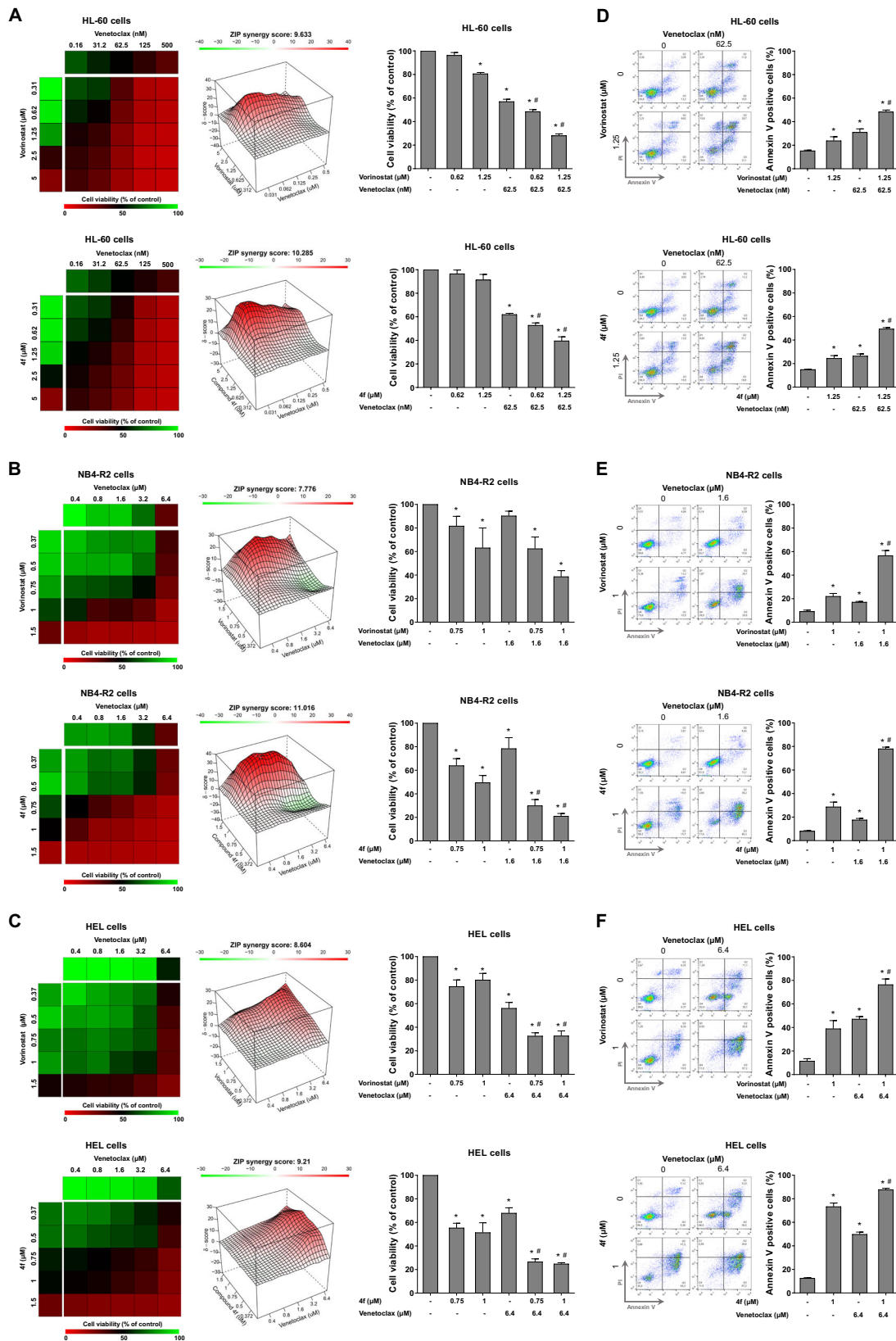
In the present study, hybrid kinase/HDAC inhibitors selectively reduced leukemia cell viability in several blood cancer models. The use of epigenetic inhibitors targeting HDAC in clinical settings began around 2006 with vorinostat for cutaneous T-cell lymphoma released [33]. Following vorinostat's promising results, other HDAC inhibitors demonstrated preclinical efficacy, leading to rapid clinical development, with several entering Phase I–III trials and being approved for hematologic malignancies [34]. For instance, belinostat showed an overall response rate of 25% and was well-tolerated in patients with cutaneous T-cell lymphoma or peripheral T-cell lymphoma [35]. Panobinostat, another HDAC inhibitor, induced histone hyperacetylation within 4 h of administration in patients (Phase I study) and reduced peripheral blood blasts in 11 patients (Phase II study), confirming its efficacy as a single agent or in combination with other drugs [34, 36–38]. While these drugs have been successful in treating hematologic disorders, none of them function as hybrid kinase/HDAC inhibitors, which could offer more potent effects by targeting additional cancer-specific pathways.

In a previous study, hybrid inhibitors combining purine-benzohydroxamate with substituted anilines or heteroaryl amines were used to inhibit kinases (including JAK1, JAK2, JAK3, BTK, CDK4, SKY, TRK $\alpha$ , PI3K $\alpha$ , and PI3K $\delta$ ) and HDACs (HDAC1 and HDAC6) in blood cancer cells. These novel molecules, synthesized by our research group, were tested and found to be potent and

specific against leukemia and lymphoma, providing chemical diversity that enhances anticancer effects by interacting with both HDACs and kinases [19]. Cancer's capacity for mutational plasticity, especially when a single target is inhibited, often leads to treatment resistance via mutations in the target or activation of compensatory mechanisms. This results in most tumors acquiring resistance within a few months [39–41]. Combination therapy involving two or more drugs that interact with multiple targets has shown success in overcoming resistance. Ongoing clinical studies, approved by the FDA, aim to evaluate the efficacy, toxicity, and safety of new multi-target drugs, including tyrosine kinase inhibitors. However, no HDAC inhibitor-tyrosine kinase inhibitor combinations have yet been approved, though they represent an important avenue for cancer treatment [42–45].

In the present study, the hybrid kinase/HDAC inhibitor **4f** showed a synergistic effect in venetoclax-resistant AML cell lines. Venetoclax, a selective BCL2 inhibitor, has shown promising responses in clinical studies and was approved by the FDA in 2020 for AML. Despite promising results, resistance often develops after months to years of treatment. BCL2 has been shown to mediate chemoresistance and enhance the survival of leukemic blast [46, 47], making new drug combinations essential [48–53]. For example, in a study of a large cohort of AML patients treated with venetoclax and azacitidine, higher rates of complete remission were observed compared to the control group [53]. Another study in newly diagnosed and relapsed/refractory FLT3-mutated AML patients showed high remission rates when venetoclax was combined with azacitidine and gilteritinib [54] (NCT04140487). DiNardo et al. reported high response rates in patients treated with venetoclax and FLAG-IDA (fludarabine, cytarabine, G-CSF, and idarubicin) in both newly diagnosed and relapsed/refractory AML cases [55]. Even with these positive results, older patients often experience higher toxicity levels, necessitating alternative therapies [22–24]. The combination of HDAC inhibitors like panobinostat with venetoclax has been shown to sensitize cytarabine-resistant AML cells and enhance the cytotoxicity of standard therapies in blood cancer experimental models [56–58]. The combination of belinostat and venetoclax in primary cells reduced cell viability, induced apoptosis, and increased mitochondrial priming in T-cell prolymphocytic leukemia [59]. Similarly, chidamide in combination with venetoclax decreased cell viability and induced apoptosis in AML cell lines and primary cells, showing tumor growth reduction and prolonged survival in mice [60]. These studies corroborate our findings and highlight the potential of combining HDAC inhibitors with venetoclax for more effective treatment [61].

Clinically, venetoclax-based therapies achieve favorable responses, such as complete remission, in approximately one-third of AML patients, highlighting the urgent need to address intrinsic resistance mechanisms [20]. HEL and NB4 cells were selected for this study due to their poor responsiveness to venetoclax, with NB4 cells exhibiting intermediate resistance and HEL cells demonstrating high resistance to this agent. Our findings suggest that even in cell models intrinsically resistant to BCL2 inhibitors, the addition of HDAC inhibitors can enhance the efficacy of these agents. Mechanistically, although HDAC inhibitors do not directly alter BCL2 expression, chromatin remodeling may



regulate the expression of other BCL2 family members or tumor suppressor genes, collectively contributing to the observed effects. For example, in HEL cells, a decrease in *BCL2* expression was accompanied by increases in *BECN1* and *BNIP3L*.

*BECN1* sequesters *BCL2*, thereby reducing its anti-apoptotic function, while *BNIP3L*, a BH3-only pro-apoptotic protein, may act as a sensitizer to apoptosis. Similarly, vorinostat treatment elevated the expression of *BNIP3*, another BH3-only pro-apoptotic



**Fig. 6 Compound 4f acts synergistically on venetoclax-induced apoptosis and is more effective than vorinostat in acute myeloid leukemia (AML) cells.** Dose-response cytotoxicity for vorinostat plus venetoclax and **4f** plus venetoclax was analyzed by methylthiazolium (MTT) assay in HL-60 (**A**), NB4-R2 (**B**) and HEL cells (**C**). AML were exposure to vehicle or graded concentrations of venetoclax and vorinostat or **4f** alone or in combination with each other for 48 h, as indicated. Values are expressed as the percentage of vehicle-treated cells. The ZIP synergy score was calculated using the SynergyFinder software (<https://synergyfinder.fimm.fi/>). Bar graphs highlight context-relevant combinations. \* $p < 0.05$  treatment versus vehicle and # $p < 0.05$  monotherapy versus combined therapy; ANOVA test and Bonferroni post-test. Results are shown as the mean of at least three independent experiments. HL-60 (**D**), NB4-R2 (**E**), and HEL (**F**) cells were labeled with APC-annexin V/propidium iodide (PI) being treated with vehicle or venetoclax and vorinostat or **4f** alone or in combination with each other for 48 h. Representative dot plots are shown for each condition. The upper and lower right quadrants (Q2 plus Q3) cumulatively contain the cell death population (annexin V+ cells). Bar graphs represent the mean  $\pm$  SD of at least three independent experiments. The  $p$  values and cell lines are indicated in the graphs; \* $p < 0.05$  treatment versus vehicle and # $p < 0.05$  monotherapy versus combined therapy; ANOVA test and Bonferroni post-test.

protein [62–64]. In addition, treatment with compound **4f** induced the expression of tumor suppressor genes involved in DNA damage responses, such as *GADD45A* and *CDKN1A*, further contributing to reduced cell viability [65, 66]. These findings underscore the potential of HDAC inhibitors to overcome intrinsic resistance to venetoclax by modulating pro-apoptotic pathways and tumor suppressor gene networks.

In a previous study, the kinases JAK2 and JAK3 emerged as potential targets of the new hybrid kinase/HDAC inhibitor being investigated in the current research [19]. Notably, higher potency was observed in HEL cells, which harbor a constitutively active JAK2<sup>V617F</sup> mutation that drives activation of the JAK2/STAT, MAPK, and PI3K/AKT pathways, promoting cellular proliferation and survival [67, 68]. Our data indicates that HDACi induces a transient inhibition of STAT3/5 phosphorylation in HEL cells, which may explain its greater potency compared to other cell lines (Supplementary Fig. 6).

In summary, purine-benzohydroxamate compounds, particularly **4f**, exhibit potent antineoplastic effects across a range of hematological malignancies, selectively reducing cell viability in neoplastic cells while sparing normal leukocytes. These effects are mediated through apoptosis induction, cell cycle arrest, and inhibition of HDAC activity, with **4f** demonstrating superior efficacy compared to vorinostat in both colony formation and differentiation assays. Additionally, **4f** modulates key genes involved in apoptosis, DNA damage, and autophagy, leading to enhanced therapeutic responses. Notably, the combination of **4f** with venetoclax significantly potentiates the reduction in cell viability, overcoming venetoclax resistance in AML models, highlighting the potential of **4f** as a promising therapeutic strategy for resistant hematological malignancies.

## MATERIAL AND METHODS

### Cell culture and inhibitors

A panel containing cellular models of hematological malignancies, including acute myeloid leukemia (AML), acute lymphoblastic leukemia (ALL), lymphoma, and multiple myeloma was used. U-937, HEL, K-562, KU812, Jurkat, Namalwa, Daudi, Raji, REH, U266, MM1.S, and MM1.R cells were provided by Prof. Sara Teresinha Olalla Saad (Hemocentro, University of Campinas, Brazil). OCI-AML3, Kasumi-1, HL-60, THP-1, MOLM-13, MV4-11, NB4, and NB4-R2 cells were provided by Prof. Eduardo Magalhães Rego (Faculdade de Medicina, University of São Paulo, Brazil). SET-2 cells were provided by Prof. Dr. Fabíola Attí de Castro (School of Pharmaceutical Sciences of Ribeirão Preto, University of São Paulo, Ribeirão Preto, Brazil). CEM and NALM6 cells were provided by Dr. Gilberto Carlos Franchi Junior (Universidade de Campinas, Campinas, Brazil). The cell lines were cultivated in culture medium recommended by the American Type Culture Collection (ATCC) or Deutsche Sammlung von Mikroorganismen und Zellkulturen (DSMZ), supplemented with fetal bovine serum and penicillin/streptomycin. The cells were maintained at 37°C, 5% CO<sub>2</sub>. Peripheral blood mononuclear cells from healthy donors (normal leukocytes) were obtained by Ficoll gradient (Sigma-Aldrich) according to the manufacturer's instructions and cultured in RPMI-1640 medium containing 30% FBS, penicillin/streptomycin, and recombinant cytokines (Peprotech Inc., Rocky Hill, NJ, USA) (30 ng/mL IL-3, 100 ng/mL IL-7, 100 ng/mL FLT3 ligand, and

30 ng/mL SCF). The study was approved by the ICB-USP Human Research Ethics Committee (Protocol: 4423074; CAAE: 39510920.1.0000.5467). Vorinostat was obtained from Sigma-Aldrich (St. Louis, MO, USA). Compounds **4d**, **4e**, and **4f** were synthesized as previously described [19]. The compounds were diluted in dimethyl sulfoxide (DMSO) (Synth, Diadema, SP, Brazil) at 50 mM and stored at –20°C. In the 'vehicle condition (0  $\mu$ M), cells were treated with an equivalent amount of DMSO. The chemical structures of HDACi are illustrated in Supplementary Fig. 7.

### Cell viability assay

Cell viability was measured using the MTT assay, according to the manufacturer's instructions (Sigma-Aldrich, St. Louis, MI, USA). Briefly,  $2 \times 10^4$  (cell lines) or  $2 \times 10^5$  cells (primary cells) per well were cultured in a 96-well plate with the appropriate culture medium and increasing concentrations of the analyzed compounds. After 24, 48, and/or 72 h of incubation, 10  $\mu$ L of a solution containing MTT at 5 mg/mL was added and incubated for 4 h at 37°C. The reaction was then stopped by adding 100  $\mu$ L of 0.1 N HCl in isopropanol. Cell viability was measured at an absorbance of 570 nm using an automatic plate reader. The experiments were performed with at least three replicates per condition, and at least three independent experiments were conducted for each condition. IC<sub>50</sub> values were calculated using nonlinear regression analysis in GraphPad Prism 8 software (GraphPad Software, Inc., San Diego, CA, USA). For combined treatment analysis, HL-60 cells were exposed to graded doses of vorinostat (0.31, 0.62, 1.25, 2.5, and 5  $\mu$ M) and venetoclax (0.16, 31.3, 62.5, 125, and 500 nM) or **4f** (0.31, 0.62, 1.25, 2.5, and 5  $\mu$ M) and venetoclax (0.16, 31.3, 62.5, 125, and 500 nM) alone or in combination for 48 h. NB4-R2 or HEL cells were exposed to graded doses of vorinostat (0.25, 0.5, 0.75, 1, and 1.5  $\mu$ M) and venetoclax (0.4, 0.8, 1.6, 3.2, and 6.4  $\mu$ M) or **4f** (0.25, 0.5, 0.75, 1, and 1.5  $\mu$ M) and venetoclax (0.4, 0.8, 1.6, 3.2, and 6.4  $\mu$ M) alone or in combination for 48 h. Data were illustrated using the Multiple Experiment Viewer (MeV) 4.9.0 software (<http://www.tm4.org/mev/>). The ZIP synergy score was calculated using the SynergyFinder software (<https://synergyfinder.fimm.fi/>).

### Cell death assay

HEL, MOLM-13, NB4-R2, or THP-1 cells ( $1 \times 10^5$  per well) were seeded in 24-well plates with vehicle, vorinostat, **4d**, **4e**, and **4f** (0.75, 1, 1.5, or 2  $\mu$ M) for 24 h.

For combined treatment, cells were exposed to vorinostat or **4f** (HL-60: 1.25  $\mu$ M, NB4-R2 and HEL: 1  $\mu$ M) and venetoclax (HL-60: 62.5 nM, NB4-R2: 1.6  $\mu$ M, and HEL: 6.4  $\mu$ M) alone or in combination for 48 h. The cells were then washed with ice-cold phosphate-buffered saline (PBS) and resuspended in a binding buffer containing 1  $\mu$ g/mL propidium iodide (PI) and 1  $\mu$ g/mL APC-labeled annexin V. All specimens were analyzed by flow cytometry (FACSCalibur; Becton Dickinson, Franklin Lakes, NJ, USA) after incubation for 15 min at room temperature in a light-protected area. Ten thousand events were recorded for each sample.

### Cell cycle assay

HEL, MOLM-13, NB4-R2, or THP-1 cells ( $1 \times 10^5$  per well) were seeded in 12-well plates with vehicle, vorinostat, or **4f** (0.75, 1, or 1.5  $\mu$ M), and then harvested after 24 h. The cells were fixed with 70% ethanol and stored at 4°C for at least 4 h. The fixed cells were then stained with PBS containing 20  $\mu$ g/mL propidium iodide (PI) and 10  $\mu$ g/mL RNase A for 30 min at room temperature in a light-protected area. DNA content distribution was determined using flow cytometry (FACSCalibur; Becton Dickinson) and analyzed with FlowJo software (TreeStar, Inc.).



### Autonomous colony formation assay

Colony formation assays were performed in semi-solid methylcellulose medium ( $1 \times 10^3$  cells/mL; MethoCult 4230; StemCell Technologies Inc., Vancouver, BC, Canada) in the presence of vehicle, vorinostat, or **4f** (0.25, 0.5, 1, 1.5, and 2  $\mu$ M). After ten days of culture, colonies were detected by adding MTT solution (5 mg/mL). Images were acquired using the G:BOX Chemi XX6 gel documentation system (Syngene, Cambridge, United Kingdom) and analyzed with ImageJ software (US National Institutes of Health, Bethesda, MD, USA).

### Cell differentiation analysis

NB4-R2 and THP-1 cells were treated with the vehicle, vorinostat or **4f** for 96 h and subjected flow cytometry and panoptic staining. After treatment, cells were collected and resuspended in PBS containing 5  $\mu$ L of anti-CD11b-PE. Following incubation in the dark for 30 min at room temperature, the samples were washed with PBS and analyzed on a FACSCalibur. Ten thousand events were acquired for each sample. For cytospin, a total of  $1 \times 10^5$  cells were adhered to microscopic slides using a cytospin (Serocyte, model 2400, FANEM, Guarulhos, Brazil) for subsequent Rosenfeld staining. Morphological analysis of the nucleus and cytoplasm was visualized using a Leica DM 2500 optical microscope, and images were acquired with LAS V4.6 software (LEICA, Bensheim, Germany).

### Western blot analysis

Total protein extraction was performed using a buffer containing 100 mM Tris (pH 7.6), 1% Triton X-100, 2 mM PMSF, 10 mM  $\text{Na}_3\text{VO}_4$ , 100 mM NaF, 10 mM  $\text{Na}_4\text{P}_2\text{O}_7$ , and 4 mM EDTA. Equal amounts of protein (15  $\mu$ g) from the samples were subjected to SDS-PAGE in an electrophoresis device, followed by electrotransfer of the proteins to nitrocellulose membranes. The membranes were blocked with 5% non-fat dry milk and incubated with specific primary antibodies diluted in blocking buffer, followed by secondary antibodies conjugated to horseradish peroxidase (HRP). Western blot analysis was performed using a SuperSignal™ West Dura Extended Duration substrate system (Thermo Fisher Scientific, Waltham, MA, USA) and a G:BOX Chemi XX6 gel documentation system (Syngene). Antibodies against acetyl-histone H3 Lys9 (#9649), histone H3 (#4499), acetyl- $\alpha$ -tubulin Lys40 (#5335),  $\alpha$ -tubulin (#2144), and GAPDH (#5174) were obtained from Cell Signaling Technology (Danvers, MA, USA). Cropped gels retain important bands, but entire gel images are available in Supplementary Fig. 8.

### Quantitative RT-PCR (qRT-PCR)

Total RNA was extracted using TRIzol reagent (Thermo Fisher Scientific), and cDNA was synthesized from 1  $\mu$ g RNA using a High-Capacity cDNA Reverse Transcription Kit (Thermo Fisher Scientific). Quantitative PCR (qPCR) was performed using a QuantStudio 3 Real-Time PCR System in conjunction with a SYBR Green system (Thermo Fisher Scientific). *HPRT1* and *ACTB* were used as reference genes. Relative quantification values were calculated using the  $2^{-\Delta\Delta CT}$  equation [69]. Expression of cell cycle-, apoptosis-, DNA damage-, and autophagy-related genes (Supplementary Table 1) was investigated in HEL cells following exposure to vehicle, vorinostat (1  $\mu$ M), or **4f** (1  $\mu$ M) for 24 h. A heatmap was generated using the Multiple Experiment Viewer (MeV) 4.9.0 software (<http://mev.tm4.org>). Differentially expressed genes with  $p > 0.05$  were used for network construction using the GeneMANIA database (<https://genemania.org/>).

### Bioinformatics

*HDAC1*, *HDAC2*, *HDAC3*, *HDAC4*, *HDAC5*, *HDAC6*, *HDAC7*, *HDAC8*, *HDAC9*, *HDAC10*, and *HDAC11* mRNA expression data from healthy donors ( $n = 13$ ) and AML ( $n = 577$ ) were obtained from Amazonia! database 2008 [70], which were generated using cDNA microarrays Affymetrix HGU133 plus 2.0 arrays. Data sets were cross-referenced using tumor-specific identification numbers. The numbers of individuals for each group are indicated. Correlation analysis was performed using the Spearman test and RStudio software (version 1.4.1717, RStudio, PBC) and the Corrplot plugin. The area under the curve (AUC) values from 165 drugs tested in ex vivo assays by the Beat AML study ( $n = 520$ ) were utilized to explore the correlation between drug response and *HDAC2*, *HDAC6*, and *HDAC8* expression [71, 72].

### Statistical analysis

Statistical analyses were performed using GraphPad Prism 8 (GraphPad Software Inc.). Mann–Whitney test, analysis of variance (ANOVA) and

Bonferroni post-test, Student *t* test, or Spearman correlation test were used, as appropriate. A  $p < 0.05$  were statistically considered.

### DATA AVAILABILITY

The data generated or analyzed in this study during the current study are available from the corresponding author on reasonable request.

### REFERENCES

- Portela A, Esteller M. Epigenetic modifications and human disease. *Nat Biotechnol.* 2010;28:1057–68.
- Dai Z, Ramesh V, Locasale JW. The evolving metabolic landscape of chromatin biology and epigenetics. *Nat Rev Genet.* 2020;21:737–53.
- Sadida HQ, Abdulla A, Marzooqi SA, Hashem S, Macha MA, Akil ASA, et al. Epigenetic modifications: Key players in cancer heterogeneity and drug resistance. *Transl Oncol.* 2024;39:101821.
- Liu R, Wu J, Guo H, Yao W, Li S, Lu Y, et al. Post-translational modifications of histones: mechanisms, biological functions, and therapeutic targets. *MedComm* (2020). 2023;4:e292.
- Cedar H, Bergman Y. Linking DNA methylation and histone modification: patterns and paradigms. *Nat Rev Genet.* 2009;10:295–304.
- Rajan PK, Udoh UA, Sanabria JD, Banerjee M, Smith G, Schade MS, et al. The role of histone acetylation-/methylation-mediated apoptotic gene regulation in hepatocellular carcinoma. *Int J Mol Sci.* 2020;21:8894.
- Yang J, Song C, Zhan X. The role of protein acetylation in carcinogenesis and targeted drug discovery. *Front Endocrinol (Lausanne).* 2022;13:972312.
- Dang F, Wei W. Targeting the acetylation signaling pathway in cancer therapy. *Semin Cancer Biol.* 2022;85:209–18.
- Shi MQ, Xu Y, Fu X, Pan DS, Lu XP, Xiao Y, et al. Advances in targeting histone deacetylase for treatment of solid tumors. *J Hematol Oncol.* 2024;17:37.
- Liang T, Wang F, Elhassan RM, Cheng Y, Tang X, Chen W, et al. Targeting histone deacetylases for cancer therapy: Trends and challenges. *Acta Pharm Sin B.* 2023;13:2425–63.
- Li Y, Seto E. HDACs and HDAC inhibitors in cancer development and therapy. *Cold Spring Harb Perspect Med.* 2016;6:a026831.
- New M, Olzscha H, La Thangue NB. HDAC inhibitor-based therapies: can we interpret the code? *Mol Oncol.* 2012;6:637–56.
- Wang P, Wang Z, Liu J. Role of HDACs in normal and malignant hematopoiesis. *Mol Cancer.* 2020;19:5.
- Wachholz V, Mustafa AM, Zeyn Y, Henninger SJ, Beyer M, Dzulklo M, et al. Inhibitors of class I HDACs and of FLT3 combine synergistically against leukemia cells with mutant FLT3. *Arch Toxicol.* 2022;96:177–93.
- Deng Y, Cheng Q, He J. HDAC inhibitors: Promising agents for leukemia treatment. *Biochem Biophys Res Commun.* 2023;680:61–72.
- Garcia-Manero G, Kazmierczak M, Wierzbowska A, Fong CY, Keng MK, Ballinari G, et al. Pracinostat combined with azacitidine in newly diagnosed adult acute myeloid leukemia (AML) patients unfit for standard induction chemotherapy: PRIMULA phase III study. *Leuk Res.* 2024;140:107480.
- Roy R, Ria T, RoyMahaPatra D, Sk UH. Single inhibitors versus dual inhibitors: role of HDAC in cancer. *ACS Omega.* 2023;8:16532–44.
- Luan Y, Li J, Bernatchez JA, Li R. Kinase and histone deacetylase hybrid inhibitors for cancer therapy. *J Med Chem.* 2019;62:3171–83.
- Waitman KB, de Almeida LC, Primi MC, Carlos J, Ruiz C, Kronenberger T, et al. HDAC specificity and kinase off-targeting by purine-benzohydroxamate anti-hematological tumor agents. *Eur J Med Chem.* 2024;263:115935.
- Pollyea DA, Amaya M, Strati P, Konopleva MY. Venetoclax for AML: changing the treatment paradigm. *Blood Adv.* 2019;3:4326–35.
- Siegel RL, Miller KD, Fuchs HE, Jemal A. Cancer statistics, 2022. *CA Cancer J Clin.* 2022;72:7–33.
- Rowe JM, Tallman MS. How I treat acute myeloid leukemia. *Blood.* 2010;116:3147–56.
- Jaramillo S, Schlenk RF. Update on current treatments for adult acute myeloid leukemia: to treat acute myeloid leukemia intensively or non-intensively? That is the question. *Haematologica.* 2023;108:342–52.
- Nagel G, Weber D, Fromm E, Erhardt S, Lubbert M, Fiedler W, et al. Epidemiological, genetic, and clinical characterization by age of newly diagnosed acute myeloid leukemia based on an academic population-based registry study (AMLSG Bio). *Ann Hematol.* 2017;96:1993–2003.
- Juliusson G, Antunovic P, Derolf A, Lehmann S, Mollgard L, Stockelberg D, et al. Age and acute myeloid leukemia: real world data on decision to treat and outcomes from the Swedish Acute Leukemia Registry. *Blood.* 2009;113:4179–87.
- Guerra VA, DiNardo C, Konopleva M. Venetoclax-based therapies for acute myeloid leukemia. *Best Pr Res Clin Haematol.* 2019;32:145–53.

27. Plass C, Oakes C, Blum W, Marcucci G. Epigenetics in acute myeloid leukemia. *Semin Oncol*. 2008;35:378–87.
28. San Jose-Eneriz E, Gimenez-Camino N, Agirre X, Prosper F. HDAC Inhibitors in Acute Myeloid Leukemia. *Cancers (Basel)* 2019;11.
29. Cai SF, Levine RL. Genetic and epigenetic determinants of AML pathogenesis. *Semin Hematol*. 2019;56:84–89.
30. Johnstone RW, Licht JD. Histone deacetylase inhibitors in cancer therapy: is transcription the primary target? *Cancer Cell*. 2003;4:13–18.
31. Berger SL, Kouzarides T, Shiekhattar R, Shilatifard A. An operational definition of epigenetics. *Genes Dev*. 2009;23:781–3.
32. Lagunas-Rangel FA, Chavez-Valencia V, Gomez-Guio MA, Cortes-Penagos C. Acute myeloid leukemia-genetic alterations and their clinical prognosis. *Int J Hematol Oncol Stem Cell Res*. 2017;11:328–39.
33. Mann BS, Johnson JR, Cohen MH, Justice R, Pazdur R. FDA approval summary: vorinostat for treatment of advanced primary cutaneous T-cell lymphoma. *Oncologist*. 2007;12:1247–52.
34. Atadja P. Development of the pan-DAC inhibitor panobinostat (LBH589): successes and challenges. *Cancer Lett*. 2009;280:233–41.
35. Foss F, Advani R, Duvic M, Hymes KB, Intratumorachai T, Lekhakula A, et al. A Phase II trial of Belinostat (PXD101) in patients with relapsed or refractory peripheral or cutaneous T-cell lymphoma. *Br J Haematol*. 2015;168:811–9.
36. Giles F, Fischer T, Cortes J, Garcia-Manero G, Beck J, Ravandi F, et al. A phase I study of intravenous LBH589, a novel cinnamic hydroxamic acid analogue histone deacetylase inhibitor, in patients with refractory hematologic malignancies. *Clin Cancer Res*. 2006;12:4628–35.
37. Gimsing P, Hansen M, Knudsen LM, Knoblauch P, Christensen IJ, Ooi CE, et al. A phase I clinical trial of the histone deacetylase inhibitor belinostat in patients with advanced hematological neoplasia. *Eur J Haematol*. 2008;81:170–6.
38. Mithraprabhu S, Kalf A, Gartlan KH, Savvidou I, Khong T, Ramachandran M, et al. Phase II trial of single-agent panobinostat consolidation improves responses after sub-optimal transplant outcomes in multiple myeloma. *Br J Haematol*. 2021;193:160–70.
39. Jiao Q, Bi L, Ren Y, Song S, Wang Q, Wang YS. Advances in studies of tyrosine kinase inhibitors and their acquired resistance. *Mol Cancer*. 2018;17:36.
40. Rotow J, Bivona TG. Understanding and targeting resistance mechanisms in NSCLC. *Nat Rev Cancer*. 2017;17:637–58.
41. Zhong L, Li Y, Xiong L, Wang W, Wu M, Yuan T, et al. Small molecules in targeted cancer therapy: advances, challenges, and future perspectives. *Signal Transduct Target Ther*. 2021;6:201.
42. Petrelli A, Giordano S. From single- to multi-target drugs in cancer therapy: when aspecificity becomes an advantage. *Curr Med Chem*. 2008;15:422–32.
43. Yao L, Mustafa N, Tan EC, Poulsen A, Singh P, Duong-Thi MD, et al. Design and synthesis of ligand efficient dual inhibitors of janus kinase (JAK) and histone deacetylase (HDAC) based on ruxolitinib and vorinostat. *J Med Chem*. 2017;60:8336–57.
44. Anighoro A, Bajorath J, Rastelli G. Polypharmacology: challenges and opportunities in drug discovery. *J Med Chem*. 2014;57:7874–87.
45. Attwood MM, Fabbro D, Sokolov AV, Knapp S, Schioth HB. Trends in kinase drug discovery: targets, indications and inhibitor design. *Nat Rev Drug Discov*. 2021;20:839–61.
46. Del Poeta G, Venditti A, Del Principe MI, Maurillo L, Buccisano F, Tamburini A, et al. Amount of spontaneous apoptosis detected by Bax/Bcl-2 ratio predicts outcome in acute myeloid leukemia (AML). *Blood*. 2003;101:2125–31.
47. Lagadinou ED, Sach A, Callahan K, Rossi RM, Neering SJ, Minhajuddin M, et al. BCL-2 inhibition targets oxidative phosphorylation and selectively eradicates quiescent human leukemia stem cells. *Cell Stem Cell*. 2013;12:329–41.
48. DiNardo CD, Pratz KW, Letai A, Jonas BA, Wei AH, Thirman M, et al. Safety and preliminary efficacy of venetoclax with decitabine or azacitidine in elderly patients with previously untreated acute myeloid leukaemia: a non-randomised, open-label, phase 1b study. *Lancet Oncol*. 2018;19:216–28.
49. DiNardo CD, Pratz K, Pullarkat V, Jonas BA, Arellano M, Becker PS, et al. Venetoclax combined with decitabine or azacitidine in treatment-naïve, elderly patients with acute myeloid leukemia. *Blood*. 2019;133:7–17.
50. Wei AH, Montesinos P, Ivanov V, DiNardo CD, Novak J, Laribi K, et al. Venetoclax plus LDAC for newly diagnosed AML ineligible for intensive chemotherapy: a phase 3 randomized placebo-controlled trial. *Blood*. 2020;135:2137–45.
51. Chua CC, Roberts AW, Reynolds J, Fong CY, Ting SB, Salmon JM, et al. Chemotherapy and venetoclax in elderly acute myeloid leukemia trial (CAVEAT): a phase Ib dose-escalation study of venetoclax combined with modified intensive chemotherapy. *J Clin Oncol*. 2020;38:3506–17.
52. Kadia TM, Reville PK, Borthakur G, Yilmaz M, Kornblau S, Alvarado Y, et al. Venetoclax plus intensive chemotherapy with cladribine, idarubicin, and cytarabine in patients with newly diagnosed acute myeloid leukaemia or high-risk myelodysplastic syndrome: a cohort from a single-centre, single-arm, phase 2 trial. *Lancet Haematol*. 2021;8:e552–e561.
53. DiNardo CD, Jonas BA, Pullarkat V, Thirman MJ, Garcia JS, Wei AH, et al. Azacitidine and Venetoclax in Previously Untreated Acute Myeloid Leukemia. *N Engl J Med*. 2020;383:617–29.
54. Short NJ, Daver N, Dinardo CD, Kadia T, Nasr LF, Macaron W, et al. Azacitidine, venetoclax, and gilteritinib in newly diagnosed and relapsed or refractory FLT3-mutated AML. *J Clin Oncol*. 2024;42:1499–508.
55. DiNardo CD, Lachowicz CA, Takahashi K, Loghavi S, Xiao L, Kadia T, et al. Venetoclax combined with FLAG-IDA induction and consolidation in newly diagnosed and relapsed or refractory acute myeloid leukemia. *J Clin Oncol*. 2021;39:2768–78.
56. Zhao J, Wu S, Wang D, Edwards H, Thibodeau J, Kim S, et al. Panobinostat sensitizes AraC-resistant AML cells to the combination of azacitidine and venetoclax. *Biochem Pharm*. 2024;228:116065.
57. Valdez BC, Li Y, Murray D, Liu Y, Nieto Y, Bashir Q, et al. Panobinostat and venetoclax enhance the cytotoxicity of gemcitabine, busulfan, and melphalan in multiple myeloma cells. *Exp Hematol*. 2020;81:32–41.
58. Schwartz J, Niu X, Walton E, Hurley L, Lin H, Edwards H, et al. Synergistic anti-leukemic interactions between ABT-199 and panobinostat in acute myeloid leukemia ex vivo. *Am J Transl Res*. 2016;8:3893–902.
59. Herbaux C, Kornauth C, Poulain S, Chong SJF, Collins MC, Valentin R, et al. BH3 profiling identifies ruxolitinib as a promising partner for venetoclax to treat T-cell prolymphocytic leukemia. *Blood*. 2021;137:3495–506.
60. Li G, Li D, Yuan F, Cheng C, Chen L, Wei X. Synergistic effect of chidamide and venetoclax on apoptosis in acute myeloid leukemia cells and its mechanism. *Ann Transl Med*. 2021;9:1575.
61. Liu E, Chen Y, Qin M, Yue K, Sun S, Jiang Y, et al. Design, synthesis, and biological activity evaluation of novel HDAC3 selective inhibitors for combination with Venetoclax against acute myeloid leukemia. *Eur J Med Chem*. 2024;276:116663.
62. Marquez RT, Xu L. Bcl-2:Beclin 1 complex: multiple mechanisms regulating autophagy/apoptosis toggle switch. *Am J Cancer Res*. 2012;2:214–21.
63. Burton TR, Gibson SB. The role of Bcl-2 family member BNIP3 in cell death and disease: NIPping at the heels of cell death. *Cell Death Differ*. 2009;16:515–23.
64. Gross A, Katz SG. Non-apoptotic functions of BCL-2 family proteins. *Cell Death Differ*. 2017;24:1348–58.
65. Palomer X, Salvador JM, Grinan-Ferre C, Barroso E, Pallas M, Vazquez-Carrera M. GADD45A: With or without you. *Med Res Rev*. 2024;44:1375–403.
66. Cazzalini O, Scovassi AI, Savio M, Stivala LA, Prosperi E. Multiple roles of the cell cycle inhibitor p21(CDKN1A) in the DNA damage response. *Mutat Res*. 2010;704:12–20.
67. Martin P, Papayannopoulou T. HEL cells: a new human erythroleukemia cell line with spontaneous and induced globin expression. *Science*. 1982;216:1233–5.
68. Machado-Neto JA, Fenerich BA, Scopim-Ribeiro R, Eide CA, Coelho-Silva JL, Dechand CRP, et al. Metformin exerts multitarget antileukemia activity in JAK2(V617F)-positive myeloproliferative neoplasms. *Cell Death Dis*. 2018;9:311.
69. Livak KJ, Schmittgen TD. Analysis of relative gene expression data using real-time quantitative PCR and the 2<sup>-</sup>(Delta Delta C(T)) Method. *Methods*. 2001;25:402–8.
70. Carrou TL, Assou S, Tondeur S, Lhermitte L, Lamb N, Reme T, et al. Amazonia: an online resource to google and visualize public human whole genome expression data. *Open Bioinforma J*. 2010;4:5–10.
71. Bottomly D, Long N, Schultz AR, Kurtz SE, Tognon CE, Johnson K, et al. Integrative analysis of drug response and clinical outcome in acute myeloid leukemia. *Cancer Cell*. 2022;40:850–64.e859.
72. Tyner JW, Tognon CE, Bottomly D, Wilmot B, Kurtz SE, Savage SL, et al. Functional genomic landscape of acute myeloid leukaemia. *Nature*. 2018;562:526–31.

## ACKNOWLEDGEMENTS

JAEGC received a fellowship from FAPESP (grant 2021/06138-0). This study was supported by grants 2021/11606-3, 2021/08260-8, 2023/12246-6, and 2024/07723-2 from the São Paulo Research Foundation (FAPESP) and grant 305758/2021-7 from Conselho Nacional de Desenvolvimento Científico e Tecnológico (CNPq). This study was financed in part by the Coordenação de Aperfeiçoamento de Pessoal de Nível Superior, Brasil (CAPES), Finance Code 001.

## AUTHOR CONTRIBUTIONS

Conceived and designed experiments: JAEGC, MTT, KL, LCA, KBW, LVCL, RPF, and JAMN. Performed the experiments: JAEGC, KL, JAMN. Analyzed the data: JAEGC, MTT, KL, LCA, KBW, LVCL, RPF, and JAMN. Wrote the paper: JAEGC and JAMN. Revised the paper: MTT, KL, LCA, KBW, LVCL, and RPF. Acquire funding: JAMN, LVCL, and RPF.

## COMPETING INTERESTS

The authors declare no competing interests.

## ETHICS

The authors conducted their research in line with the best practices and codes of conduct of relevant professional bodies and/or national and international regulatory bodies. All methods were performed in accordance with the relevant guidelines and regulations. All specimens were obtained with informed consent from healthy donors, and the study was approved by the ICB-USP Human Research Ethics Committee (Protocol: 4423074; CAAE: 39510920.1.0000.5467).

## ADDITIONAL INFORMATION

**Supplementary information** The online version contains supplementary material available at <https://doi.org/10.1038/s41420-025-02446-4>.

**Correspondence** and requests for materials should be addressed to João Agostinho Machado-Neto.

**Reprints and permission information** is available at <http://www.nature.com/reprints>

**Publisher's note** Springer Nature remains neutral with regard to jurisdictional claims in published maps and institutional affiliations.



**Open Access** This article is licensed under a Creative Commons Attribution 4.0 International License, which permits use, sharing, adaptation, distribution and reproduction in any medium or format, as long as you give appropriate credit to the original author(s) and the source, provide a link to the Creative Commons licence, and indicate if changes were made. The images or other third party material in this article are included in the article's Creative Commons licence, unless indicated otherwise in a credit line to the material. If material is not included in the article's Creative Commons licence and your intended use is not permitted by statutory regulation or exceeds the permitted use, you will need to obtain permission directly from the copyright holder. To view a copy of this licence, visit <http://creativecommons.org/licenses/by/4.0/>.

© The Author(s) 2025